

Propagation of laser-generated heat pulses in crystals at low temperature: Spatial filtering of ballistic phonons

M. Greenstein, M. A. Tamor, and J. P. Wolfe

*Physics Department, University of Illinois at Urbana-Champaign, Urbana, Illinois 61801
and Materials Research Laboratory, University of Illinois at Urbana-Champaign, Urbana, Illinois 61801*

(Received 21 June 1982)

At low temperatures, energy deposited on a crystal surface by a laser pulse or an Ohmic heater can flow rapidly away from the excitation point by ballistic phonon propagation. However, at higher excitation levels, evidence has been reported that a portion of the absorbed energy is trapped near the excitation region, creating a "hot spot." Thin-film bolometers on the opposite crystal face have been used to detect phonons emitted from the excitation region. Unfortunately, a subset of the phonons that strike the detector has been scattered in flight so the usual heat-pulse signals are not a reliable measure of the local dynamics of the excitation region. To remedy this, we have developed a technique for investigating both the time and spatial dependence of a laser-induced heat pulse. The method uses the phonon-focusing effect to discriminate between phonons that propagate directly from the excitation region to the detector and those that are scattered in the bulk of the sample. Prior studies of heat pulses following pulsed laser excitation of Ge and Si revealed, at high powers, a long-lived ($\sim 10\text{-}\mu\text{s}$) flux of phonons following the sharp ballistic pulse. Our spatial filtering technique shows that a major portion of this delayed flux in Ge is spatially very diffusive, but a short-lived component of the delayed flux emanates directly from the excitation region. We conclude that in Ge at 1.8 K, a $0.1\text{-}\mu\text{s}$ laser pulse produces a local storage of energy decaying with a time constant ~ 0.1 to $1.5\ \mu\text{s}$, depending on the excitation level. This local energy storage also appears in metal-coated Ge, heavily-doped Ge, and metal-coated GaAs and LiF, indicating that the observed energy storage is not electronic. A simple scattering model that uses local melting as a temperature calibration explains the data in terms of a localized heat-storage effect.

I. INTRODUCTION

In recent years a great deal of attention has been paid to the effect of intense laser pulses on semiconductor surfaces. Optical excitation of a semiconductor generates energetic free carriers that cool to the lattice temperature via phonon emission. A broad range of phonon frequencies is generated, although high-frequency acoustic and optical phonons are generally expected to be short lived ($\tau < 1\ \mu\text{s}$). In pure semiconductor crystals at low temperatures, the mean free path of lower-frequency ($\nu \lesssim 500\ \text{GHz}$) acoustic phonons that are generated as the byproduct of this carrier thermalization can exceed 1 cm. Thus these acoustic phonons may traverse the sample unscattered. In a crystal such as Ge, ballistic propagation is spatially anisotropic, due to phonon focusing.¹ In this paper we show that the sharp anisotropies associated with phonon focusing can be used as a "spatial filter" to isolate the time evolution of the nonthermal phonon

population very close to the excitation region.

An early experimental investigation of the phonon fluxes following intense laser excitation of Ge at low temperatures was reported by Hensel and Dynes.² For low-power focused laser excitation, the ballistic phonon pulses which traversed the sample were equal in duration to the excitation pulse (300 ns). However, at high excitation power the sharp ballistic phonon pulses acquired a very broad tail of up to $\sim 10\text{-}\mu\text{s}$ duration. This broad tail following the ballistic pulses has since been reported by other workers.³⁻⁵ To explain this apparently long-lived source of phonons, Hensel and Dynes proposed the concept of a "hot spot," in which phonon-phonon scattering greatly reduced the acoustic-phonon mean free path near the excitation region. These authors estimated a characteristic radius of $600\ \mu\text{m}$ and a temperature of 8.5 K for the hot spot.

Our interest in this problem has arisen from experiments in which electron-hole droplets (EHD) are created in Ge at $T = 1.8\ \text{K}$ by an intense laser

pulse. Electron-hole droplets are effectively transported into the crystal by nonequilibrium phonon fluxes. The droplet velocity is a unique “detector” of phonon flux. Time- and space-resolved droplet luminescence experiments indicate that an effective phonon source persists with 1–2- μs time constant after a 0.1- μs laser excitation pulse.⁶ However, when detected by a bolometer, the phonon signal with the same excitation intensity persisted for about 10 μs , a time similar to those reported in Refs. 2–5.

To resolve this apparent discrepancy a closer look at the persistent phonon flux is necessary. We have devised a simple technique that takes advantage of phonon focusing to *spatially* discriminate between those phonons that propagate directly from the excitation region to the detector, and those phonons that are delayed by multiple scattering in the bulk of the crystal. This method enables us to selectively detect the component of the delayed phonon signal which is due to energy storage at the excitation region. Phonons that are delayed by multiple scattering in the bulk of the crystal are subtracted away.

Briefly, we find that energy storage occurs over a region of lateral size comparable to the laser spot (60 μm), and that this storage region can be extremely hot. The local temperature of the storage region may be roughly calibrated by raising the excitation level sufficiently to locally melt the sample. The evolution of heat in this highly nonequilibrium situation is quite complicated, involving phonon-phonon and phonon-defect scattering. The frequency distribution of phonons changes in time and space due to down conversion of high-frequency phonons.⁷ Our heat-pulse results for pure Ge and several other crystals compare favorably to a qualitative model containing these basic features.

II. EXPERIMENTAL RESULTS

The experimental method is a variation of the ballistic phonon imaging technique of Northrop and Wolfe.⁸ Phonons are detected by a smaller granular Al bolometer (60 \times 80 μm^2) evaporated directly onto a crystal surface. The primary sample, a 1-cm cube of ultrapure single crystal Ge, was cooled in a liquid-He immersion cryostat to the superconducting transition temperature of the bolometer, $T = 1.8$ K. A Q-switched Nd:YAG (yttrium aluminum garnet) laser with a 100-ns pulse width full-width half maximum (FWHM) and 2-kHz repetition rate was used to excite a polished surface. For initial alignment the laser beam was x - y raster scanned across

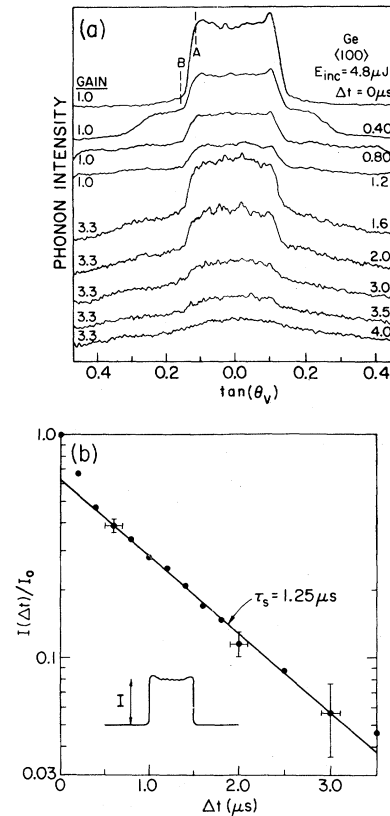


FIG. 1. Time dependence of the STA phonon singularity structure in Ge near the $\langle 100 \rangle$ direction. (a) A set of traces of the phonon intensity as a function of propagation direction for several delay times. Here, $\tan(\theta_v) = 0.0$ corresponds to the $\langle 100 \rangle$ direction and $\Delta t = 0$ corresponds to the ballistic time of flight. The traces are offset vertically for display. The additional shoulders in the intensity profile at $\Delta t = 0.40$ and 0.80 μs are due to the longer time of flight for ballistic STA phonons in those propagation directions. (b) Plot of the singularity intensity (defined in the lower left inset) as a function of time. $I_0 \equiv I(\Delta t = 0)$. The singularity intensity decays exponentially with a 1.25- μs time constant.

the crystal surface opposite the detector. A boxcar integrator was used to select the propagation time corresponding to the time of flight across the crystal of ballistic phonons that are emitted during the laser pulse. A two-dimensional ballistic phonon image similar to Fig. 2 in Ref. 8 was obtained in this manner.

Next, the time evolution of the phonon-focusing pattern was measured in order to determine what portion of the delayed phonon signal actually exhibited phonon focusing. The laser spot was scanned across the slow transverse acoustic (STA) phonon-focusing singularities located near the $\langle 100 \rangle$ direction. This was repeated for several time delays

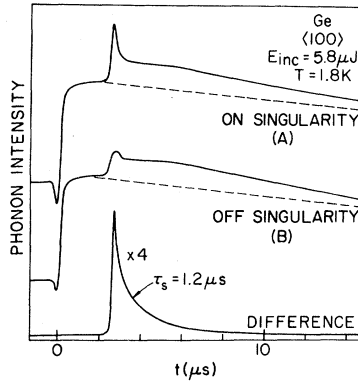


FIG. 2. Spatial filtering of ballistic phonons generated by optical excitation in Ge. By subtracting two phonon time traces at slightly different propagation angles [denoted by *A* and *B* in Fig. 1(a)] the time dependence of phonon storage at the excitation point is determined. The sharp step in the signals in the top two traces at $t=0$ corresponds to photons emitted by carrier recombination. The dashed lines represent a calculated background due to EHD recombination with a 40- μ s decay constant.

(boxcar gate delays) following the excitation. Figure 1(a) shows a series of such scans, where $\Delta t=0$ defines the STA ballistic time of flight across the crystal. The sharp jump in phonon-signal intensity at $\tan\theta_0 = \pm 0.15$ marks the STA phonon singularity.⁸

The important thing to notice is that the singularity structure persists for a time considerably longer than the excitation pulse length (100 ns). This implies that there exists a local source of phonons very near the excitation point for times well after the light pulse has ceased. In Fig. 1(b) the decay of the singularity structure [*A* minus *B* intensities in Fig. 1(a)] is shown to be approximately exponential, with a value $\tau_s = 1.25 \mu$ s. We refer to those phonons that are detected at $\Delta t=0$ as "prompt" and those arriving later as "delayed." Figure 1(a) also contains information about the size of the phonon source, as indicated by the sharpness of the intensity step at the singularity. The spatial width of this step does not change in time over the 3.5 μ s for which it is observed, giving an upper limit of 150 μ m for the size of the phonon source.

Figure 1(a) shows, in addition to the sharp singularity structure, a broad background signal which persists for many microseconds after the excitation pulse. This signal must arise from phonons which have scattered in the bulk of the crystal. To further examine the sources of the phonons detected at various times, we employed a transient recorder/signal averager (10 ns/channel) to record the time behavior of the total phonon signal for a

given propagation direction. First, a time trace was recorded for a laser position (phonon propagation direction) corresponding to point *A* in Fig. 1(a). From this time trace, the trace corresponding to point *B* in Fig. 1(a) was subtracted. A pair of such traces and their difference, taken for excitation of a polished Ge surface, is shown in Fig. 2. It should be noted that the sharp step in the signal at $t=0$ is due to photons from electron-hole droplet recombination luminescence, which decays with a 40- μ s time constant (dashed line). Above this luminescence background, the major features of the "on" and the "off" singularity traces are very similar to traces from Refs. 2–5, i.e., a long tail (~ 10 - μ s duration) appears after the ballistic pulse. However, when these two phonon traces are subtracted, their difference reveals the 1.2- μ s effective storage time, consistent with that observed in Fig. 1(b). This is the spatial filtering technique.

The principle of the subtraction is quite simple. Ballistic phonons, prompt or delayed, that travel unscattered from source to detector obey the phonon-focusing distribution. However, phonons that undergo bulk scattering do not retain the sharp focusing pattern of the ballistic phonons.⁹ The subtraction of the on and off traces at slightly different propagation directions simply removes the scattered phonon component of the total signal detected by the bolometer. Thus, the delayed phonon signal in the difference trace is a direct measure of the energy storage at the excitation region. Phonons that are delayed in leaving the excitation region and subsequently scattered in the bulk are also subtracted away by this technique, as is the luminescence background. By subtracting time traces of spatially adjacent points—separated by about 1° in propagation direction—the source-detector geometry is kept nearly constant. A good check on the validity of this technique is the high degree of accuracy with which the signal baseline is restored after subtraction.

We suspect that most of the signals previously attributed to a long-lived (10 μ s) phonon source are actually due to scattering in the bulk of the sample and not storage at the excitation region. The phonons that have been scattered in flight are not a reliable measure of the local dynamics of the excitation region. In this vein, we point out the work of Pomerantz and von Gutfeld.¹⁰ These authors found that the sharp pulses due to ballistic phonon propagation in Si and Ge could be dramatically broadened by impurity doping. By intentionally introducing extensive bulk scattering they observed phonon signals that look remarkably similar to

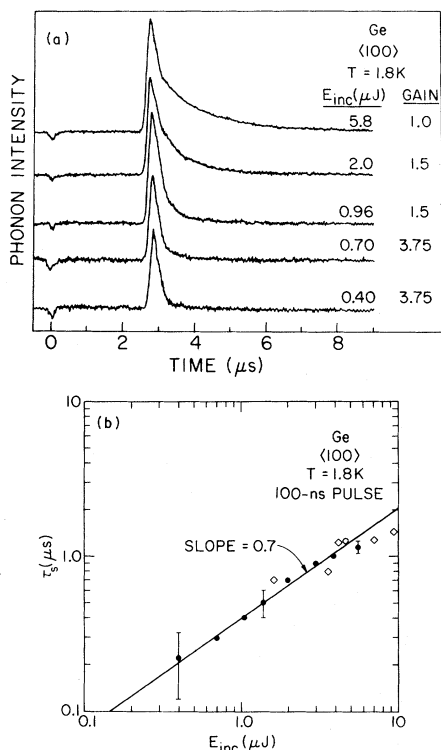


FIG. 3. Excitation dependence of the phonon-source decay time τ_s as determined by the spatial filtering technique. (a) Difference traces on pure Ge. (b) Plot of τ_s as a function of excitation level. The open circle at $E_{\text{inc}} = 4.8 \mu\text{J}$ is obtained from Fig. 1(b). The open diamonds are from Fig. 7(a) for doped Ge:Mg.

those in Refs. 2–5. However, a small fraction of the delayed phonon signal is due to localized energy storage. For a $0.1\text{-}\mu\text{s}$ excitation pulse, this component of the signal has a storage time of ~ 0.1 to $1.5 \mu\text{s}$, increasing with the excitation level as shown in Fig. 3. These phonon-source lifetimes are in agreement with those determined from the EHD experiments,⁶ resolving the apparent discrepancy mentioned earlier. We now consider the form in which the energy is stored.

One possibility is that the energy storage is in the form of photoexcited carriers. To test this hypothesis, a $600\text{-}\text{\AA}$ Cu film was evaporated onto the excitation surface of the Ge sample. Figure 4 shows the on- and off-singularity signals and their difference for this case. Nearly all of the luminescence signal has been eliminated by this Cu film, indicating very little direct optical excitation, yet the difference signal is very similar to that in Fig. 2. This is a clear indication that direct excitation of hot free carriers and a subsequent carrier thermalization process is not required for the observed energy storage. This result implies that the

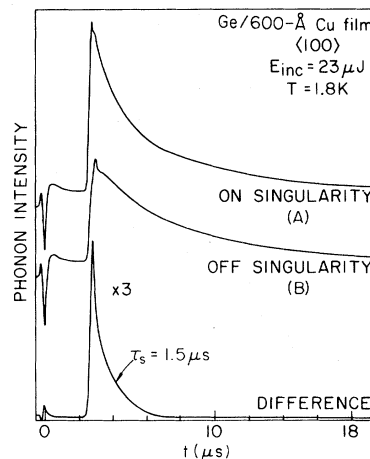


FIG. 4. Spatial filtering of ballistic phonons generated in a $600\text{-}\text{\AA}$ Cu film on Ge. The Cu film eliminates almost all of the photoexcitation, yet very similar phonon storage is still observed.

observed energy storage is purely thermal.

To further test the hypothesis of electronic energy storage, three systems with different electronic properties were tested: (1) heavily doped Ge:Mg, (2) GaAs with 600\AA of Cu, and (3) LiF with 1800\AA of Cu. In the Ge:Mg sample almost no luminescence was detected, indicating very short carrier lifetimes. Yet, the storage times were very similar to those in pure Ge. The results from the Ge:Mg sample will be discussed in Sec. III in the context of melting. Similar effects were observed in the GaAs sample. Figure 5 shows the result of the spatial filtering in LiF. Although the energy storage mechanism appears to be weaker in LiF than in Ge, the effect is still clearly observable. In

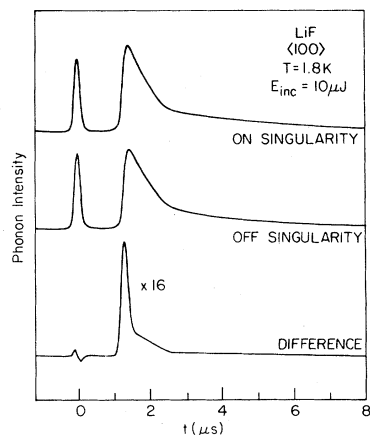


FIG. 5. Spatial filtering in LiF with an $1800\text{-}\text{\AA}$ overcoat of Cu. The sharp values at $t = 0$ is due to light from the laser pulse and establishes the system response time.

LiF, an insulator, carrier participation in the energy storage is also unlikely. All of these materials exhibit phonon storage times which monotonically increase from ~ 100 ns at low power to nearly $1 \mu\text{s}$ at higher power.

III. DISCUSSION

We suggest the following simple model which describes the major features of the data. Under intense laser excitation a heated region is formed with lifetime τ_s and lateral size comparable to the excitation spot ($\lesssim 60 \mu\text{m}$). Within this heated region, phonon-phonon scattering produces a phonon distribution roughly described by a temperature well above the bulk crystal temperature. The existence of this hot region is supported by the observed increase in τ_s with power level. For simplicity, we consider this region to radiate phonons as a Planck source, with a local temperature dependent on the excitation level. Figure 6 shows the frequency distribution of phonons emitted from Planck sources of several different temperatures. As the excitation level is increased, the relative number of high-frequency phonons increases.¹¹

The fate of these emitted phonons depends radically on their frequency, because the mean free path of phonons in Ge at low temperatures is limited by isotope scattering. The scattering time is calculated

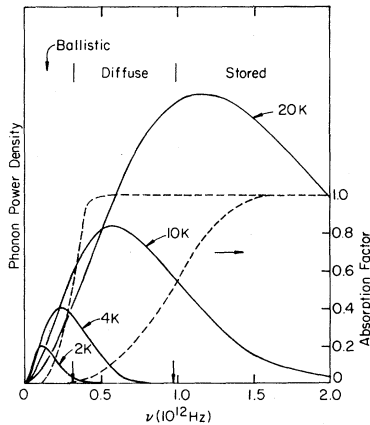


FIG. 6. Ballistic propagation, diffusive propagation, and storage regimes of the phonon system. A schematic view of these three regimes is presented by plotting a series of Planck spectra at different temperatures and the phonon absorption factor (see text) as a function of phonon frequency ν . The absorption factor, plotted for $l=100 \mu\text{m}$ and 1 cm , delineates the boundaries between the three regimes.

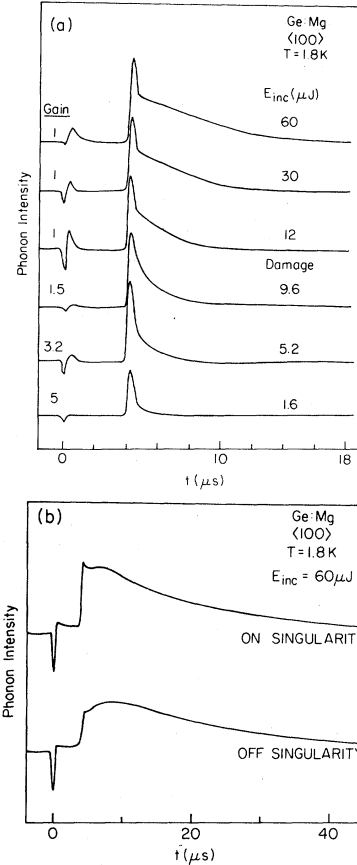


FIG. 7. Spatial filtering in Ge:Mg showing phonon storage up to and through the damage threshold. (a) Difference traces above and below the threshold for permanent, visible damage. Above the damage threshold (between 9.6 and $12 \mu\text{J}$ here) the traces change character and are no longer simply exponential. The values of τ_s obtained here below $9.6 \mu\text{J}$ are plotted as open diamonds in Fig. 3. (b) Raw phonon traces at $60 \mu\text{J}$. Note the change in the time scale.

to be $\tau^{-1} = Av^4$, where $A = 1.5 \times 10^{-41} \text{ sec}^3$ from Ref. 12, and ν is the phonon frequency. In Fig. 6 the dashed curves are the absorption factor,

$$\alpha(\nu) = 1 - \exp(-Av^4 l / V_s),$$

for two path lengths, $l = 1 \text{ cm}$ and $100 \mu\text{m}$, with V_s the phonon velocity.

Phonons with frequency greater than about 10^{12} Hz scatter within only $100 \mu\text{m}$ of the source and hence are quite localized. Down conversion of high-frequency phonons near the excitation point produces low-frequency phonons which escape the heated region and are detected as the delayed ballistic signal. Phonons with frequencies in the range 200 GHz to 1 THz have mean free paths between $100 \mu\text{m}$ and 1 cm . They leave the source region

and scatter and/or down convert before reaching the detector. These phonons produce the spatially diffuse phonon signal which remains for $\sim 10 \mu\text{s}$ after the ballistic phonon pulse. As the temperature of the heated region increases beyond 4 K, the number of these diffusive phonons far exceeds the number of low-frequency ballistic phonons. This would account for the increasing relative intensity of the 10- μs tail at higher excitation levels.

To obtain an estimate of the actual peak temperatures achieved in these phonon experiments, we increased the excitation pulse energy sufficiently to locally melt the sample. Figure 7(a) shows a set of spatially filtered bolometer traces for uncoated Ge:Mg up to and through the threshold for visible damage. The increase in τ_s is evident here. Between pulse energies of 9.7 and 12 μJ surface damage was first observed. For energies above this damage threshold the character of the difference traces changes; the tail is no longer exponential. Figure 7(b) gives the raw on and off phonon signals for $E_{\text{inc}} = 60 \mu\text{J}$. In this case an actual peak in the diffuse tail is observed.

For a pulse energy of $\sim 10 \mu\text{J}$, we know that a peak temperature of 1200 K, the melting point of Ge, is reached. Over most of the range in pulse energy in Fig. 3, the heated region is in the temperature regime of constant heat capacity ($T \gtrsim 200 \text{ K}$), where the initial temperature varies linearly with the laser power. This saturation in specific heat is due to the increasing population of dispersive phonons near the zone boundary.¹³ These zone-edge phonons have low group velocities and high scattering rates, both of which contribute to the heat storage effect.

The melting effect can also be used to estimate the depth of the heated region. The available 10 μJ raises a small volume of Ge to $T_m = 1200 \text{ K}$. Assuming that just below the melting threshold the heated volume is the same as during melting, the penetration depth will be given by

$$d = \frac{E_{\text{abs}}}{C_v \pi \rho^2 T_m}, \quad (1)$$

where E_{abs} is the absorbed laser energy ($E_{\text{abs}} \approx 0.6 E_{\text{inc}}$), C_v is the specific heat of Ge ($C_v \approx 2 \times 10^7 \text{ erg/cm}^3 \text{ K}$), and ρ is the radius of the laser spot. For $\rho \approx 30 \mu\text{m}$ in our experiments, this formula gives a heat penetration depth of only 1 μm . This very strong thermal localization is consistent with results of recent experiments studying laser annealing.¹⁴ The small penetration depth also implies that the heated region will be in the regime of constant heat capacity ($T \gtrsim 200 \text{ K}$) for pulse en-

ergies as low as 2 μJ .

The rough calibration of initial temperature with pulse energy makes possible some simple modeling of the heat storage. The simplest approximation is that all of the phonons above some cutoff frequency are effectively confined to the heated region. It is easy to estimate the total phonon energy that lies above this critical frequency. For an isotropic system, the total energy density ϵ above a minimum wave vector k_{min} is given by

$$\epsilon(k_{\text{min}}, T) = \frac{\hbar}{(2\pi)^3} \int_{k_{\text{min}}}^{k_0} \frac{k^2 \omega(k)}{e^{\hbar\omega(k)/k_B T} - 1} dk, \quad (2)$$

where k_0 is the zone-edge wave vector. The effects of dispersion near the zone edge are included here by using the standard approximation,

$$\omega(k) = V_s k_0 \left[\frac{2}{\pi} \right] \sin \left[\frac{k}{k_0} \frac{\pi}{2} \right]. \quad (3)$$

With $k_0 \approx 10^8 \text{ cm}^{-1}$ and the speed of sound $V_s = 3.5 \times 10^5 \text{ cm/s}$, the integral in Eq. (2) can be evaluated numerically.

With the assumption that the total integrated signal of the delayed ballistic phonons is proportional to the total stored energy, we can compare the data to the model integral. Figure 8 shows the total integrated prompt and delayed ballistic signals over a wide range in pulse energy. Data from both pure Ge (Fig. 3) and doped Ge:Mg (Fig. 7) are used here. The melting threshold is characterized by an abrupt increase in the stored energy, and a saturation in the

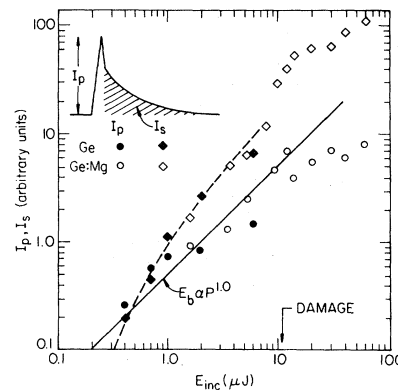


FIG. 8. Total integrated prompt I_p and stored I_s phonon signals as a function of incident pulse energy. The inset defines these two quantities. Since I_p has a constant duration equal to the laser pulse width, I_p is proportional to the prompt signal height as shown. The dashed curve is from Eq. (2) for I_s . The solid line indicates the expected linear dependence of I_p on excitation level.

ballistic signal. The onset of melting appears to lie at $\sim 9 \mu\text{J}$, below the damage threshold. By defining $9 \mu\text{J}$ to correspond to $T = 1200 \text{ K}$, the model curve from Eq. (2) (the dashed line) may be superposed on the data. The results of the calculation were found to be quite insensitive to the choice of lower-cutoff frequency. Values between 1.0 and 3.0 THz produced nearly indistinguishable curves. The close correspondence between the data and model indicate that the (spatially filtered) delayed ballistic signal is a good measure of the total heat storage. It also suggests that the concept of phonon confinement above a critical frequency is valid.

The model also predicts that the prompt ballistic signal should be linear in pulse energy. The data in Fig. 8 are not inconsistent with this prediction. The saturation of the prompt signal above $10 \mu\text{J}$ may be due to the thermal decoupling of the melted region from the underlying crystal. As the surface melts the ballistic and diffusive phonons are also trapped, and the storage efficiency increases. Both these effects seem to be present in the data of Fig. 8. From these results we may conclude that the observed phonon storage associated with the spatially filtered signal is due to the slow cooling of a very thin heated layer at the surface of the crystal.

Our simple model does not address the power dependence of the storage time. Further progress on this problem may require extensive modeling of

the localization and down-conversion processes. The predictions of these models may then be compared with bolometer data in order to determine the relative importance of the various localization mechanisms. We believe that the spatial filtering technique will be useful in providing such data.

In conclusion, we have demonstrated a spatial filtering technique for phonons that allows direct observation of ballistic phonons that are initially stored at the excitation region. The very long tails in the phonon signals reported in the past are mostly artifacts of bulk phonon scattering processes. We observe a shorter, about $1 \mu\text{s}$, energy storage time that is due to localized phonon storage. The general features of the data are accounted for by a power-dependent frequency distribution emitted from the excitation region and the known mass-defect scattering in Ge.

ACKNOWLEDGMENTS

We wish to thank G. A. Northrop for help in the initial setup of this experiment and for several useful discussions. This project was supported in part by the National Science Foundation under Grant No. DMR-80-24000 and by the Materials Research Laboratory Grant No. DMR-80-20250.

- ¹B. Taylor, H. J. Maris, and C. Elbaum, *Phys. Rev. B* **3**, 1462 (1971); J. H. Maris, *J. Acoust. Soc. Am.* **50**, 812 (1971).
- ²J. C. Hensel and R. C. Dynes, *Phys. Rev. Lett.* **39**, 969 (1977).
- ³V. S. Bagaev, G. Bel'skaya-Levandovskaya, M. M. Bonch-Osmolovskii, T. I. Galkina, S. Y. Levandovskii, G. N. Mikhailova, A. G. Poyarkov, and H. Jung, *Zh. Eksp. Teor. Fiz.* **77**, 2117 (1979) [*Sov. Phys.—JETP* **50**, 1013 (1979)].
- ⁴G. A. Northrop, M. Greenstein, and J. P. Wolfe, *Bull. Amer. Phys. Soc.* **26**, 311 (1981).
- ⁵R. E. Horstman and J. Wolter, in *Proceedings of the International Conference on Phonon Physics* [*J. Phys. (Paris)* **42**, C6-813 (1981)].
- ⁶M. A. Tamor, M. Greenstein, and J. P. Wolfe (unpublished).
- ⁷W. E. Bron and W. Grill, *Phys. Rev. B* **16**, 5305 (1977); **16**, 5315 (1977).
- ⁸G. A. Northrop and J. P. Wolfe, *Phys. Rev. Lett.* **43**, 1424 (1979); *Phys. Rev. B* **22**, 6196 (1980). See also J. C. Hensel and R. C. Dynes, *Phys. Rev. Lett.* **43**, 1033

(1979).

- ⁹Phonons that undergo a small angle scattering propagate with a direction and a total time of flight the same as that of unscattered phonons of the same mode. Thus these phonons are indistinguishable from ballistic phonons.
- ¹⁰M. Pomerantz and R. J. von Gutfeld, in *Proceedings of the Ninth International Conference on the Physics of Semiconductors, Moscow, 1968*, edited by S. M. Ryvkin (Nauka, Leningrad, 1968).
- ¹¹Hensel and Dynes, Ref. 2, suggested alternatively that the distribution of phonons emitted from a "hot spot" is relatively independent of excitation level, since the surface of the hot spot would radiate at a temperature $T \approx 8.5 \text{ K}$, given by its surface temperature.
- ¹²J. Callaway, *Phys. Rev.* **113**, 1046 (1959).
- ¹³C. Kittel, *Introduction to Solid State Physics*, 5th ed. (Wiley, 1976, New York), Chap. 5.
- ¹⁴G. J. Galvin, M. O. Thompson, J. W. Mayer, R. B. Hammond, N. Paulter, and P. S. Peerey, *Phys. Rev. Lett.* **48**, 33 (1982).